Supporting Information

Specific protein detection using designed DNA carriers and nanopores

Nicholas A. W. Bell and Ulrich F. Keyser

Cavendish Laboratory, University of Cambridge, JJ Thomson Ave, Cambridge, CB3 0HE, United Kingdom

DNA carrier synthesis

All enzymes and m13mp18 DNA were purchased from New England Biolabs. All oligonucleotides were purchased from Integrated DNA Technologies. The DNA carrier was synthesised using the 7249 base single stranded DNA m13mp18 virus genome. Firstly, a 39 base oligonucleotide with sequence

5' –TCTAGAGGATCCCCGGGTACCGAGCTCGAATTCGTAATC – 3'

was hybridised to the scaffold by mixing the following

20 µL m13mp18 DNA (250ng/µL)
4 µL 10x New England Biolabs cutsmart buffer
1 µL oligonucleotide (100µM)
14 µL deionised water

Followed by heating to 65°C and linearly cooling to 25°C in a thermocycler over 40 minutes. 0.5µL of BamHI-HF and 0.5µL EcoRI-HF (each 100000 units/ml) were then added to the reaction mixture followed by incubation at 37°C for 1 hour. The cut m13mp18 DNA was then immediately purified using a Machery-Nagel NucleoSpin gel and PCR Clean-up kit.

Having cut the scaffold, the double stranded DNA carrier was formed by mixing together the following

4 µL cut m13mp18 DNA (100nM)
20 µL oligonucleotide mix (each oligo 200nM)
4 µL 100mM $MgCl_2$
1.6 µL 100mM Tris-HCl (pH=8), 10mM EDTA
10.4 µL deionised water

And heated to 70°C followed by linearly cooling to 25°C over 1 hour. The sequences of all oligonucleotides used in the various DNA carrier designs is given at the end of the supporting information.

Each oligonucleotide is present at a 10 times excess to the cut m13mp18 DNA in the reaction mixture to ensure a high yield of correctly formed structures. The excess oligonucleotides were removed using Amicon Ultra 100 kDa cut-off centrifugal filters (Millipore) – a procedure commonly used for purification of DNA origami nanostructures from excess oligonucleotides. The protocol was 6 rounds of centrifuging at 3000g and 4°C with each round lasting 10 minutes. The sample was then recovered by turning the filter upside down and centrifuging for 2 minutes at 1000g.

Gel analysis revealed that the staple band was removed by this purification procedure (see Supporting Figure 2). The purified DNA carrier was then aliquoted and stored at -20°C before use.

DNA carrier synthesis yield and staple removal

The m13mp18 scaffold produced by New England Biolabs (NEB) is primarily circular and NEB estimate that >90% of molecules are in the circular form with the remaining molecules being in the linear. The linear molecules are inherently due to the purification process (see NEB website for further details).

The base sequence position of the nick which creates a linear DNA is presumably random. Therefore during the scaffold cutting process these linear molecules will be cut at random positions and produce fragments as in Supporting Figure 1. This therefore produces a small background in our experiments.

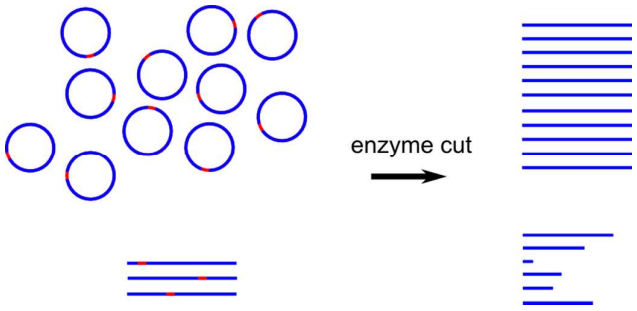

Supporting Figure 1: Cutting of the m13mp18 results in a small amount of fragments due to the presence of linear molecules in the m13mp18 before cutting. The recognition site is represented in red on the blue DNA strand.

Agarose gel electrophoresis was used to assess the yield of full length double stranded DNA carrier and to check the removal of excess oligonucleotides by Amicon filtration. In Supporting Figure 2 lanes 2 and 3 show there is a slight shift due to the cutting of the m13mp18 which removes 21 bases. Lane 4 shows the double stranded DNA carrier after formation but without excess oligonucleotide purification. The main band runs between the 6kbp and 8kbp markers on the ladder and there is a diffuse band at the bottom of the gel due to the excess oligonucleotides. Lane 5 shows the double stranded DNA carrier after excess oligonucleotide purification. The absence of the staple band in lane 4 confirms that the excess oligonucleotides are removed using the filtration protocol.

Lane 6 shows a sample which was made in order to estimate the amount of linear molecules in the m13mp18 before cutting. For this sample the m13mp18 (uncut) was hybridised with the complete oligonucleotide mix (with the same protocol as the DNA carrier). Therefore the circular scaffolds will form a circular double strand and the already linear scaffolds will form a linear double strand. Indeed we observe that there is a faint band that runs at the same speed as the DNA carrier which can be attributed to linear strands of 7249 bp and a strong band due to circular 7249 bp. Using the ImageJ gel analysis tool the mass percentage of DNA in the linear band was calculated to be 11%. Since the mass of each DNA in the circular and linear bands is the same this means that ~11% of the m13mp18 is present as linear molecules in qualitative agreement with the >90% specified by NEB. Therefore after

cutting, hybridising complementary oligos and purifying ~22 % of DNA carriers are not the full length. We decided that this background was acceptable within the experiments since the selection of DNA carrier events based on event charge deficit should preclude most fragments. In future, to create highly pure samples in future the DNA carrier could be purified from an agarose gel. However this typically gives lower yields than Amicon filtration.

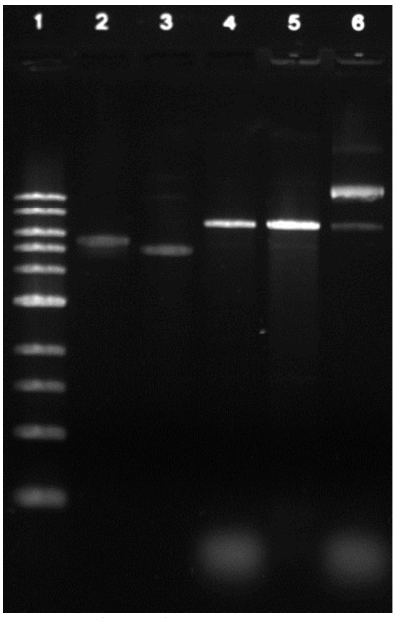

Supporting Figure 2: Agarose gel to quantify synthesis quality and yield. The 1% agarose gel was run at 80V for 90 mins in 1xTAE buffer. Lane 1 = New England Biolabs 1kb ladder, Lane 2 = m13mp18 before cutting, Lane 3 = m13mp18 after cutting, Lane 4 = DNA carrier before staple purification, Lane 5 = DNA carrier after staple purification, Lane 6 = Primarily circular DNA carrier made without cutting the m13mp18.

A rough estimation of DNA carrier lengths was also made by atomic force microscopy. Supporting Figure 3 shows a large area scan of 10.5 μm x 10.5 μm of the purified DNA carrier absorbed onto mica. The length of each isolated polymer chain was traced out using ImageJ and is shown in units of microns. A 7228 bp length of double stranded DNA should have a contour length of 2.5 μm (assuming 0.34 nm/bp). We observe most DNA strands have a slightly shorter length of 1.9-2.4 μm which we interpret as due to the large scale image not accurately tracking all the kinks in the DNA and therefore underestimating the true contour. The percentage of lengths less than 1.9 μm is 24% (10/41) which roughly agrees with the estimate of 22% of DNA lengths shorter than the full length made above using gel electrophoresis data.

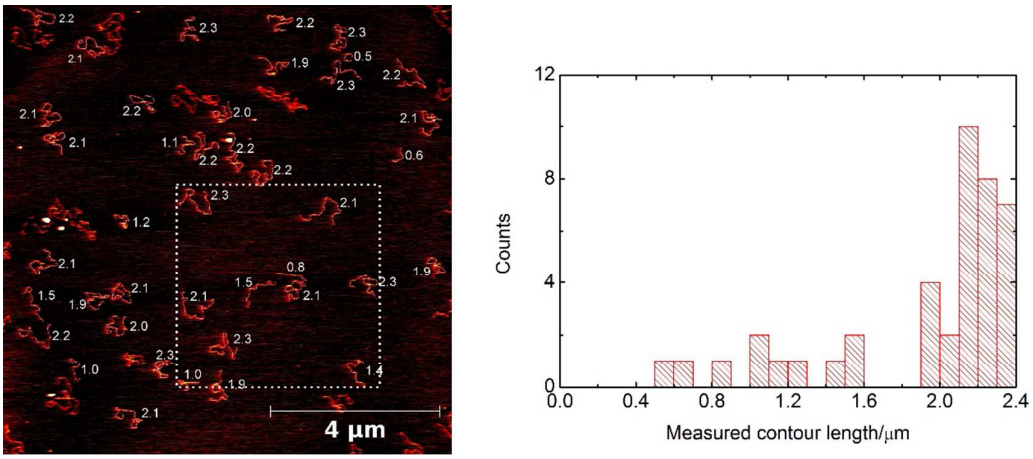

Supporting Figure 3: Left: Large area AFM of DNA carrier absorbed onto mica. Polymer chain lengths are marked in microns. The dotted area is shown at higher magnification in Figure 1c in the main text. Right: Histogram of lengths measured.

Glass nanopore fabrication

Quartz capillaries with inner diameter 0.2 mm, outer diameter 0.5 mm and containing a 0.05 mm fused filament were purchased from Sutter Instruments. Each capillary was cleaned by sonication in acetone followed by drying under nitrogen. The capillaries were then pulled to a form a glass nanopore using a Sutter P-2000 capillary puller with the following settings:

Heat	Filament	Delay	Velocity	Pull
480	0	170	25	200

Supporting Table 1: Sutter P-2000 settings for forming glass nanopores.

Each glass nanopore was integrated into a microfluidic chip as previously described[1].

Determination of nanopore geometry and estimation of DNA current change

A sample of 10 glass nanopores, made with the settings in Supporting Table 1, was imaged to determine typical values for the diameter and taper angle at the tip. Imaging was performed using the in-lens detector of a Zeiss FEG Sigma-VP SEM at 2-3 kV acceleration voltage. Supporting Figure 4 shows a view of a glass nanopore at a large scale in (a) and with inner and outer diameters marked in (b). On a few occasions we were able to obtain sufficient resolution and contrast to be able to differentiate between the walls and the inside of the nanopore. The ratio of ID:OD (inner diameter: outer diameter) at the tip is to a good approximation the same as that of the capillary before pulling where ID = 0.2 mm and OD = 0.5 mm. This constant wall thickness ratio has also been observed in larger pores made by glass capillary pulling[2]. Therefore when the inside diameter was not visible, we inferred the inner diameter by measuring the outer diameter and assuming a ID:OD ratio of 0.4. This analysis gives values of $d_i = 15 \pm 3$ nm (mean ± s.d., n=10).

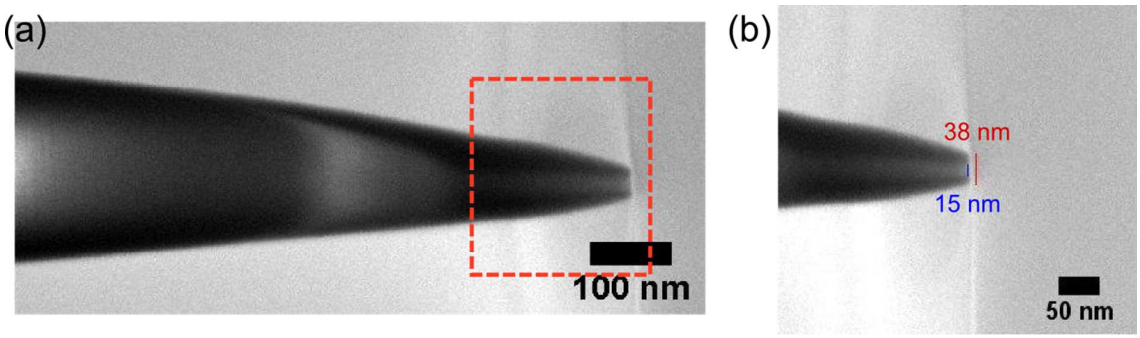

Supporting Figure 4: SEM images of a typical glass nanopore prepared using the settings given in Supporting Table 1. As the glass thins out at the tip, contrast is visible between the walls and the inside of the nanopore.

We analysed SEM images and found two taper angles were needed to accurately describe the 3D glass nanopore geometry. The first taper angle is determined from the first 100 nm from the tip. The second taper angle is determined by the next 600 nm as indicated in Supporting Figure 5a and assumed to continue on infinitely.

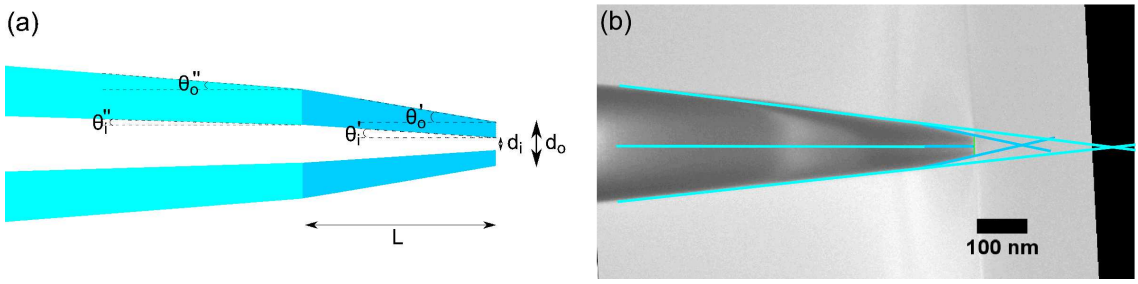

Supporting Figure 5: (a) Assumed geometry of a glass nanopore. Two cones in series (with two taper angles) are used. L is taken to be 100 nm. The light blue cone is assumed to continue indefinitely to the left. (b) Same as Supporting Supporting Figure 4a but with the outer angles of the two tapers as indicated.

The resistance of the first 100 nm length cone is given by

$$R'_{Cone} = \frac{4L}{\sigma\pi d_i(d_i + 2Ltan\theta'_i)}$$

And the infinite cone assumed to form the rest of the nanopore has a resistance given by

$$R''_{Cone} = \frac{2}{\sigma\pi(d_i + 2Ltan\theta'_i)tan\theta''_i}$$

There is also a contribution from the access resistance at the nanopore tip which can be modelled by a planar disk[3] and is given by

$$R_{Access} = \frac{1}{2\sigma d_i}$$

Therefore the total resistance is given by summing the contributions from the two cones and the access resistance

$$R_{Nanopore} = \frac{4L}{\sigma\pi d_i(d_i + 2Ltan\theta_i')} + \frac{2}{\sigma\pi(d_i + 2Ltan\theta_i')tan\theta_i''} + \frac{1}{2\sigma d_i}$$

We can infer the inner taper angles from the measured outer taper angles using the approximation that the ID:OD ratio remains constant at 0.4 along the whole length and therefore

$$\tan(\theta_i) = \alpha\tan(\theta_o)$$

Where θ_i is the inner angle, θ_o is the outer angle and α is the ratio ID:OD = 0.4.

This SEM model of the 3D geometry can be compared with our observed current change due to the DNA translocation. The resistance of the two taper geometry with an infinite cylindrical rod of radius a running through the centre (Supporting Figure 6) is given by

$$R_{Nanopore\ with\ DNA} = \frac{1}{2\sigma\pi atan\theta_i'}\left(ln\frac{2Ltan\theta_i' + d_i - 2a}{2Ltan\theta_i' + d_i + 2a} - ln\frac{d_i - 2a}{d_i + 2a}\right) - \frac{1}{2\sigma\pi atan\theta_i''}ln\frac{d_i + 2Ltan\theta_i' - 2a}{d_i + 2Ltan\theta_i' + 2a} + \frac{1}{2\sigma d_i}$$

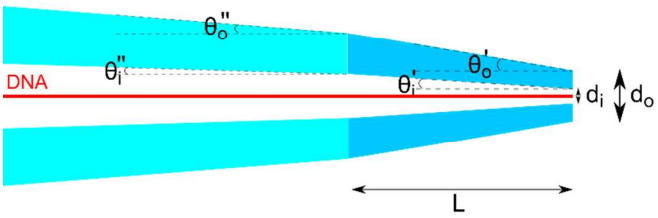

Supporting Figure 6: Estimation of current change due to passage of long DNA through the glass nanopore. The DNA is assumed to pass through the centre of the glass nanopore and to be a cylindrical rod.

Substituting in the mean values from SEM of d_i = 15 nm, θ_i' = 0.092 rad, θ_i'' = 0.046 rad and using our conditions of L = 100 nm, σ = 184 mS/cm and a radius of B-DNA of 1.25 nm gives a predicted current change

$$\Delta I = \frac{V}{R_{Nanopore}} - \frac{V}{R_{Nanopore\ with\ DNA}}$$

Of $\Delta I = 105\ pA$ at 600 mV. This agrees well with the current change values observed for the DNA carrier in the main text and indicates an accurate geometrical model.

Ionic current recording and analysis

All experiments were performed with a buffer of either 10 mM Tris (pH = 8), 1 mM EDTA, 4M LiCl or 10 mM Tris (pH = 8), 1 mM EDTA, 4M LiCl , 5 mM $MgCl_2$ in the sample reservoir. The applied voltage was always 600 mV and this typically gave a few DNA carrier

translocations per second for a DNA carrier concentration of 1 nM. Ionic current was recorded using Ag/AgCl electrodes and an Axopatch 200B amplifier. The Axopatch 200B output was filtered with an external 8-pole Bessel filter at 49.9 kHz and digitised at 250 kHz.

In an initial step to remove noisy data traces, we automatically remove any section of trace where the standard deviation in 3 seconds was greater than 25 pA. This is typically due to transient, non-specific protein or DNA sticking to the nanopore. For event threshold detection we then zero the baseline ionic current level by fitting a cubic polynomial to every 0.5 seconds of trace. We then count an event when the ionic current passes a threshold of 100 pA from this zeroed baseline level and measure the begin and end of the event as where the current crosses 30 pA (30 pA is chosen rather than 0 pA since DNA translocations through conical glass nanopores give a slow decay as the DNA moves away at the end of the translocation). The one exception to the 100 pA threshold level is Supporting Figure 10 and Supporting Figure 11 where a 60 pA threshold is used for protein only translocations. For Figure 1 in the main text and Supporting Figures 7-9 all recorded events from the 100 pA threshold condition are shown. For Figures 2-5 in the main text and later Figures in the supporting information, we do further event selection as detailed in a later section of this supporting information "Determination of DNA carrier events and selection of events beginning and ending with one DNA strand".

Comparison of translocations of 7 kbp purified DNA plasmid with 7.2kbp DNA carrier
We performed a comparison between the 7.2 kbp DNA carrier and a commercially available, chromatography-purified 7 kbp double strand (NoLimits, Thermo Scientific). Supporting Figure 7 shows experiments using four separate nanopores to measure the 7 kbp purified plasmid. We observe a very similar pattern of event scatter plot with a main band showing a characteristic mean event current inversely proportional to event duration. The percentage of translocations with low values of ECD is smaller than for the 7.2 kbp DNA carrier which is as expected due to the presence of fragments in the 7.2 kbp DNA carrier sample. We also show in Supporting Figure 8 three repeats of Figure 1f, g in the main text showing the reproducibility of the DNA carrier translocations.

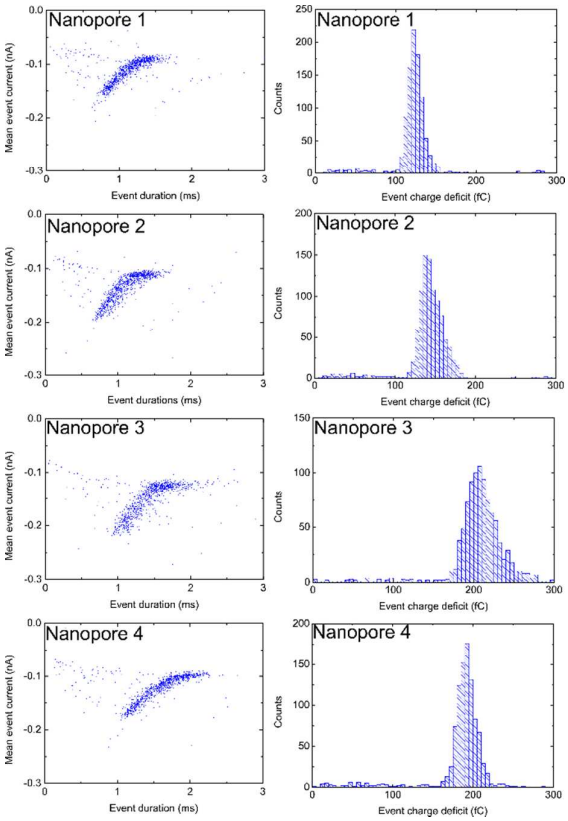

Supporting Figure 7: 7 kbp plasmid fragment translocations in 1xTE, 4M LiCl at 600 mV applied potential. Experiments on four nanopores showing the event scatter plot and event charge deficit for the first 1000 translocations.

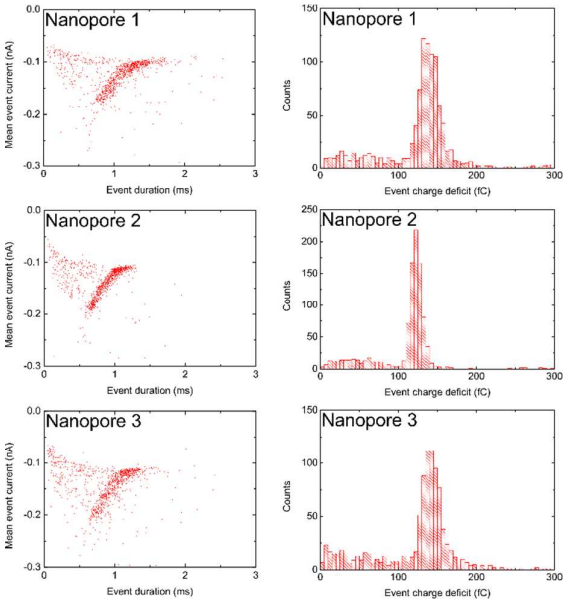

Supporting Figure 8: Three repeats of the translocation of the 7.2 kbp DNA carrier without any oligonucleotide modifications (as in Figure 1f, g in the main text). Each scatter plot and associated ECD histogram shows the first 1000 recorded events.

Translocations of m13mp18 before oligonucleotide hybridisation

Supporting Figure 9 shows typical translocation of m13mp18 DNA after cutting at BamHI and EcoRI restriction sites but before hybridizing the 190 oligonucleotides needed to from the DNA carrier. The scatter plot shows data from the first 1000 translocation events. Clearly we observe a significantly different translocation signature compared to the double stranded DNA carrier. The cut m13mp18 DNA shows a short sub-ms event duration and large amplitude current blockage. This reflects the compact globular shape of m13mp18 ssDNA compared to the extended coil-like double stranded DNA carrier as shown by the AFM images in Figure 1 of the main text. The shape of these translocations agrees with previous solid state nanopore measurements[4].

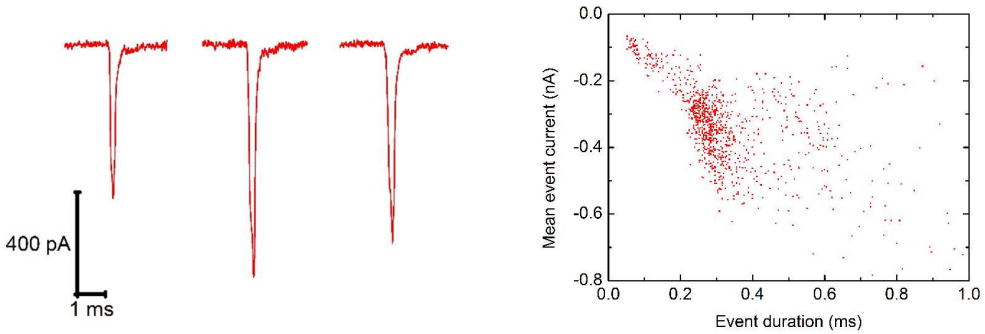

Supporting Figure 9: Left: Three typical translocations of m13mp18 ssDNA through a glass nanopore with 1xTE, 4M LiCl buffer and 600 mV applied potential. Right: Scatter plot of mean event current against duration for first 1000 translocations.

Translocations of streptavidin and anti-digoxigenin only

Supporting Figure 10 shows typical translocations of streptavidin only through glass nanopores at 600 mV applied voltage in 1x TE, 4M LiCl. The concentration was 500 nM. In common with previous solid state nanopore experiments we measure a scatter plot where the events are cut-off by the detection threshold which was set at 60 pA. Similarly Supporting Figure 11 shows statistics of translocations of anti-digoxigenin antibody only at 500 nM concentration.

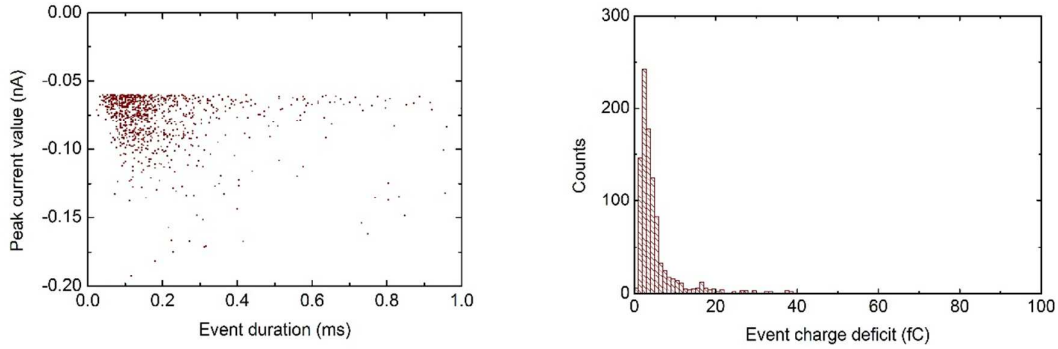

Supporting Figure 10: Translocations of streptavidin only through a glass nanopore. The peak current threshold was 60 pA and the first 1000 translocations are shown. Left: event scatter, right: ECD histogram.

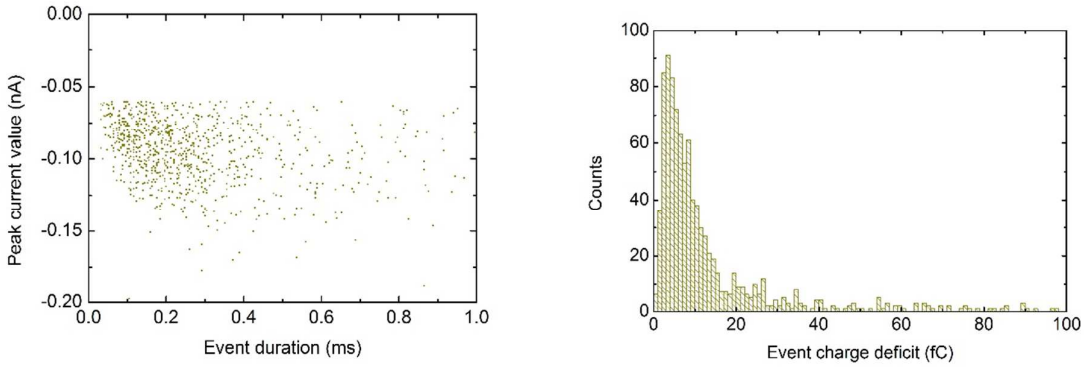

Supporting Figure 11: Translocations of anti-digoxigenin antibody only through a glass nanopore. The peak current threshold was 60 pA and the first 1000 translocations are shown. Left: event scatter, right: ECD histogram.

Determination of DNA carrier events and selection of events beginning and ending with one DNA strand

For Figures 2-5 in the main text the DNA carrier events we needed to measure only the translocation of full length DNA carriers which begin and end with one DNA strand. Therefore the following protocol was used.

1) First we recorded all events crossing 100 pA as described in the "Ionic current recording and analysis" section above. We then plotted the event charge deficit (ECD) histogram of all events with a 5 fC bin width. Crucially, the peak due to the DNA carrier typically occurs at ~100 fC to 200 fC (Supporting Figure 8) and is therefore easily discernible from the protein translocation ECD which is mainly <20 fC (Supporting Figure 10 and Supporting Figure 11). We then fit a Gaussian function to the ECD peak and select only the events that have ECD value in the range of $\mu \pm 2\sigma$ where μ is the peak value and σ is the Gaussian standard deviation. Supporting Figure 12 shows an example ECD histogram with the DNA carrier peak labelled.

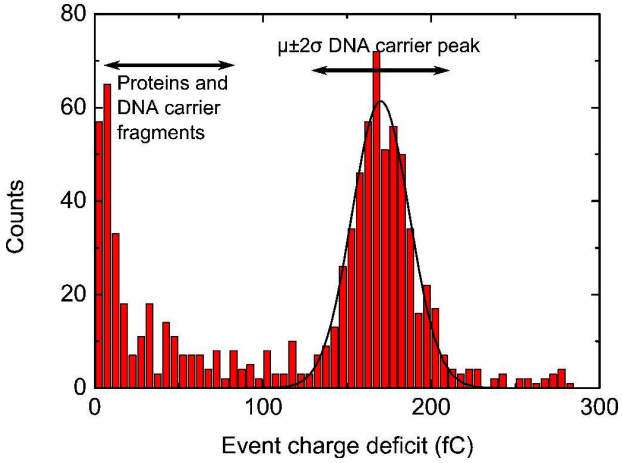

Supporting Figure 12: In stage 1 the ECD histogram is plotted and only events within $\mu \pm 2\sigma$ are retained. This particular example is an ECD histogram for one nanopore using the 3B+mix2 configuration in Figure 4 in the main text.

2) After selecting only full length DNA carrier events in Stage 1, in Stage 2 we select only events beginning and ending with one DNA strand. To do this we plot an all points histogram of the recorded events after stage one selection and fit a Gaussian to the one DNA strand peak (Supporting Figure 13). The centre of this Gaussian determines the one DNA strand level. We then reject events where the current level passes 1.5 times the one DNA strand level in the first 300 µs or last 300 µs of the event see Supporting Figure 14. Supporting Figure 15 shows the scatter plot before and after each selection stage.

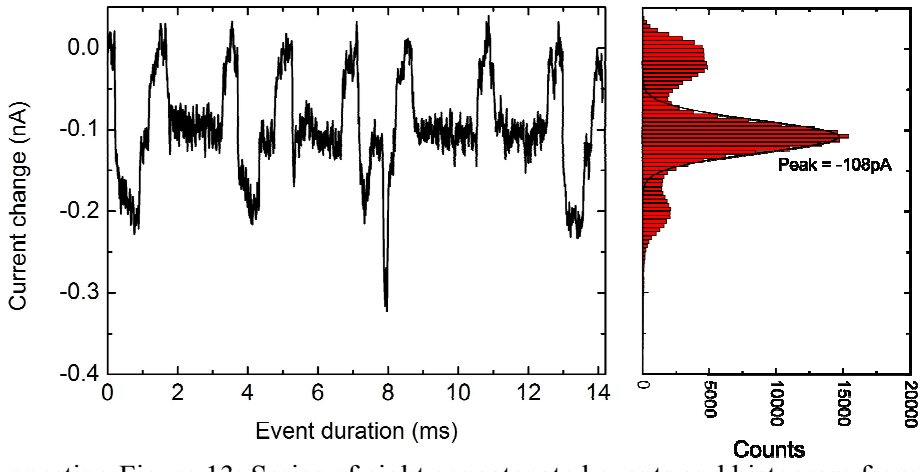

Supporting Figure 13: Series of eight concatenated events and histogram from all points of all events showing one DNA strand level peak at 108 pA.

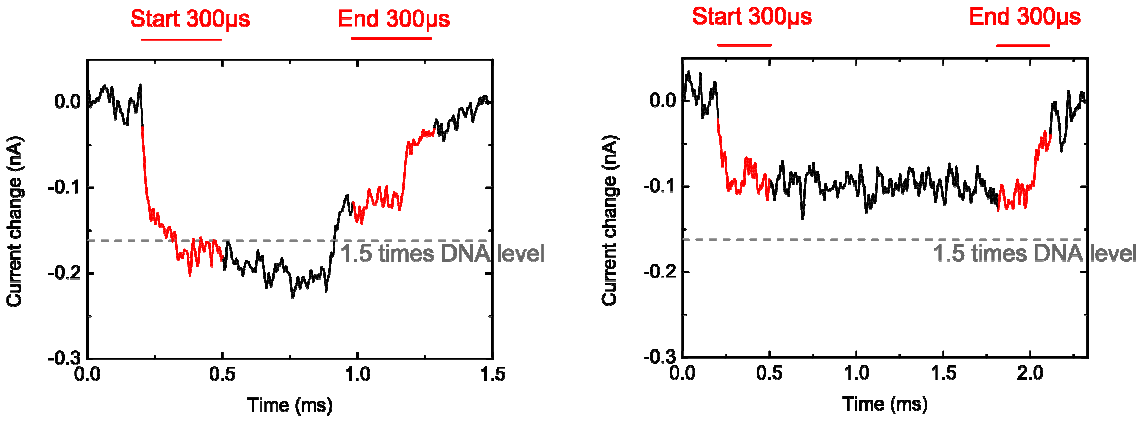

Supporting Figure 14: Examples of selection based on current at start 300 µs and end 300 µs. The event on the left crosses the 1.5 times DNA level in the start 300 µs and is therefore discarded. The event on the right does not cross either the threshold during the start 300 µs or end 300 µs and is therefore not discarded.

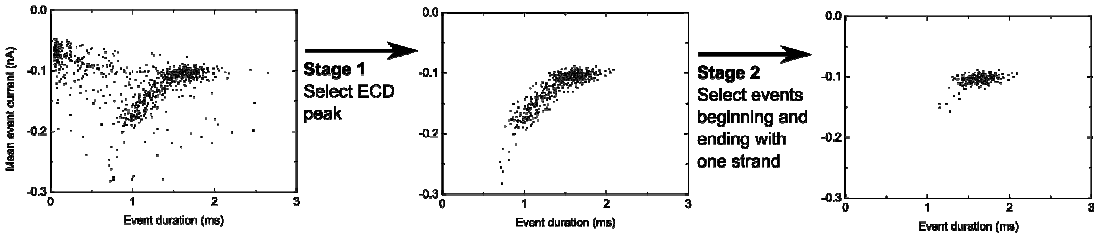

Supporting Figure 15: Progression showing scatter plot recorded from all events, events after stage 1 selection and events after stage 2 selection. The number of events decreases left to right from 917 to 517 to 236.

Raw data on detection efficiency (Figure 3b in main text)

The following tables show the number of events after stage 1 and stage 2 selection for the different thresholds given in Figure 3.

1) **5 Biotin (5B) design**

Nanopore number	Events after stage 1 and 2 selection	Events crossing 40 pA threshold in central 400 µs	Events crossing 50 pA threshold in central 400 µs	Events crossing 60 pA threshold in central 400 µs
1	71	71	71	71
2	271	268	266	262
3	69	68	68	68

Supporting Table 2: 5B design threshold figures for Figure 3.

2) **3 Biotin (3B) design**

Nanopore number	Events after stage 1 and 2 selection	Events crossing 40 pA threshold in central 400 µs	Events crossing 50 pA threshold in central 400 µs	Events crossing 60 pA threshold in central 400 µs
1	140	113	103	85
2	96	90	90	85
3	88	85	84	82
4	26	25	25	25
5	60	56	55	53

Supporting Table 3: 3B design threshold figures for Figure 3. (Figure 2h (3B) in main text shows histograms from the three nanopores which gave the highest numbers of events after stage 1 and 2 selection.)

3) **1 Biotin (1B) design**

Nanopore number	Events after	Events crossing	Events crossing	Events crossing

	stage 1 and 2 selection	40 pA threshold in central 400 µs	50 pA threshold in central 400 µs	60 pA threshold in central 400 µs
1	**75**	**37**	**16**	**11**
2	**84**	**44**	**21**	**13**
3	**166**	**85**	**45**	**27**

Supporting Table 4: 1B design threshold figures for Figure 3.

4) **0 Biotin (0B) design**

Nanopore number	Events after stage 1 and 2 selection	Events crossing 40 pA threshold in central 400 µs	Events crossing 50 pA threshold in central 400 µs	Events crossing 60 pA threshold in central 400 µs
1	**259**	**26**	**22**	**19**
2	**263**	**22**	**19**	**16**
3	**82**	**4**	**4**	**4**
4	**990**	**77**	**55**	**44**
5	**308**	**12**	**9**	**7**
6	**186**	**6**	**4**	**4**

Supporting Table 5: 0B design threshold figures for Figure 3.

Raw data on % of translocations showing positive protein spikes (Figure 4b in main text)

The following tables show the raw data for the experiments in Figure 4.

1) **3 biotin modified (3B) DNA carrier + streptavidin, β-lactoglobulin, β-galactosidase, lysozyme**

Nanopore number	Events after stage 1 and 2 selection	Number events crossing 50 pA in central 400 µs
1	**34**	**27**
2	**59**	**59**
3	**45**	**38**
4	**97**	**82**

Supporting Table 6: 3B + mix1 threshold crossing statistics.

2) **3 biotin modified (3B) DNA carrier + BSA, β-lactoglobulin, β-galactosidase, lysozyme**

Nanopore number	Events after stage 1 and 2 selection	Number events crossing 50 pA in central 400 µs
1	531	53
2	62	5
3	59	5
4	236	47

Supporting Table **7:** 3B + mix2 threshold crossing statistics.

3) **Unmodified (0B) DNA carrier + streptavidin, β-lactoglobulin, β-galactosidase, lysozyme**

Nanopore number	Events after stage 1 and 2 selection	Number events crossing 50 pA in central 400 µs
1	100	10
2	22	2
3	23	1
4	42	7

Supporting Table 8: 0B + mix1 threshold crossing statistics.

4) **Unmodified (0B) DNA carrier + BSA, β-lactoglobulin, β-galactosidase, lysozyme**

Nanopore number	Events after stage 1 and 2 selection	Number events crossing 50 pA in central 400 µs
1	32	1
2	46	7
3	301	31
4	60	12

Supporting Table 9: 0B + mix2 threshold crossing statistics.

Raw data on detection efficiency for anti-digoxigenin (Figure 5e in main text)

Nanopore number	Events after stage 1 and 2	Events crossing 40 pA threshold	Events crossing 50 pA threshold	Events crossing 60 pA threshold

	selection	in central 400 µs	in central 400 µs	in central 400 µs
1	**194**	**138**	**129**	**103**
2	**30**	**22**	**22**	**18**
3	**24**	**22**	**22**	**20**

Supporting Table 10: Statistics for threshold crossing with one digoxigenin binding site (Figure 5e in main text).

Synthesised oligonucleotide sequences

The following set is the basic oligonucleotide sequences without any modifications. The four thymine overhangs at either end are indicated in red.

Oligo no	Sequence	Length
1	TTTTCGTAATCATGGTCATAGCTGTTTCCTGTGTGAAATTGTTATC	46
2	CGCTCACAATTCCACACAACATACGAGCCGGAAGCATA	38
3	AAGTGTAAAGCCTGGGGTGCCTAATGAGTGAGCTAACT	38
4	CACATTAATTGCGTTGCGCTCACTGCCCGCTTTCCAGT	38
5	CGGGAAACCTGTCGTGCCAGCTGCATTAATGAATCGGC	38
6	CAACGCGCGGGGAGAGGCGGTTTGCGTATTGGGCGCCA	38
7	GGGTGGTTTTTCTTTTCACCAGTGAGACGGGCAACAGC	38
8	TGATTGCCCTTCACCGCCTGGCCCTGAGAGAGTTGCAG	38
9	CAAGCGGTCCACGCTGGTTTGCCCCAGCAGGCGAAAAT	38
10	CCTGTTTGATGGTGGTTCCGAAATCGGCAAAATCCCTT	38
11	ATAAATCAAAAGAATAGCCCGAGATAGGGTTGAGTGTT	38
12	GTTCCAGTTTGGAACAAGAGTCCACTATTAAAGAACGT	38
13	GGACTCCAACGTCAAAGGGCGAAAAACCGTCTATCAGG	38
14	GCGATGGCCCACTACGTGAACCATCACCCAAATCAAGT	38
15	TTTTTGGGGTCGAGGTGCCGTAAAGCACTAAATCGGAA	38
16	CCCTAAAGGGAGCCCCCGATTTAGAGCTTGACGGGGAA	38
17	AGCCGGCGAACGTGGCGAGAAAGGAAGGGAAGAAAGCG	38
18	AAAGGAGCGGGCGCTAGGGCGCTGGCAAGTGTAGCGGT	38
19	CACGCTGCGCGTAACCACCACACCCGCCGCGCTTAATG	38
20	CGCCGCTACAGGGCGCGTACTATGGTTGCTTTGACGAG	38
21	CACGTATAACGTGCTTTCCTCGTTAGAATCAGAGCGGG	38
22	AGCTAAACAGGAGGCCGATTAAAGGGATTTTAGACAGG	38
23	AACGGTACGCCAGAATCCTGAGAAGTGTTTTTATAATC	38
24	AGTGAGGCCACCGAGTAAAAGAGTCTGTCCATCACGCA	38
25	AATTAACCGTTGTAGCAATACTTCTTTGATTAGTAATA	38
26	ACATCACTTGCCTGAGTAGAAGAACTCAAACTATCGGC	38
27	CTTGCTGGTAATATCCAGAACAATATTACCGCCAGCCA	38
28	TTGCAACAGGAAAAACGCTCATGGAAATACCTACATTT	38
29	TGACGCTCAATCGTCTGAAATGGATTATTTACATTGGC	38
30	AGATTCACCAGTCACACGACCAGTAATAAAAGGGACAT	38
31	TCTGGCCAACAGAGATAGAACCCTTCTGACCTGAAAGC	38
32	GTAAGAATACGTGGCACAGACAATATTTTTGAATGGCT	38
33	ATTAGTCTTTAATGCGCGAACTGATAGCCCTAAAACAT	38
34	CGCCATTAAAAATACCGAACGAACCACCAGCAGAAGAT	38
35	AAAACAGAGGTGAGGCGGTCAGTATTAACACCGCCTGC	38
36	AACAGTGCCACGCTGAGAGCCAGCAGCAAATGAAAAAT	38
37	CTAAAGCATCACCTTGCTGAACCTCAAATATCAAACCC	38
38	TCAATCAATATCTGGTCAGTTGGCAAATCAACAGTTGA	38
39	AAGGAATTGAGGAAGGTTATCTAAAATATCTTTAGGAG	38
40	CACTAACAACTAATAGATTAGAGCCGTCAATAGATAAT	38
41	ACATTTGAGGATTTAGAAGTATTAGACTTTACAAACAA	38
42	TTCGACAACTCGTATTAAAATCCTTTGCCCGAACGTTAT	38
43	TAATTTTAAAAGTTTGAGTAACATTATCATTTTGCGGA	38
44	ACAAAGAAACCACCAGAAGGAGCGGAATTATCATCATA	38
45	TTCCTGATTATCAGATGATGGCAATTCATCAATATAAT	38
46	CCTGATTGTTTGGATTATACTTCTGAATAATGGAAGGG	38
47	TTAGAACCTACCATATCAAAATTATTTGCACGTAAAAC	38
48	AGAAATAAAGAAATTGCGTAGATTTTCAGGTTTAACGT	38
49	CAGATGAATATACAGTAACAGTACCTTTTACATCGGGA	38
50	GAAACAATAACGGATTCGCCTGATTGCTTTGAATACCA	38
51	AGTTACAAAATCGCGCAGAGGCGAATTATTCATTTCAA	38
52	TTACCTGAGCAAAAGAAGATGATGAAACAAACATCAAG	38
53	AAAACAAAATTAATTACATTTAACAATTTCATTTGAAT	38
54	TACCTTTTTTAATGGAAACAGTACATAAATCAATATAT	38
55	GTGAGTGAATAACCTTGCTTCTGTAAATCGTCGCTATT	38
56	AATTAATTTTCCCTTAGAATCCTTGAAAACATAGCGAT	38
57	AGCTTAGATTAAGACGCTGAGAAGAGTCAATAGTGAAT	38
58	TTATCAAAATCATAGGTCTGAGAGACTACCTTTTTAAC	38
59	CTCCGGCTTAGGTTGGGTTATATAACTATATGTAAATG	38
60	CTGATGCAAATCCAATCGCAAGACAAAGAACGCGAGAA	38
61	AACTTTTTCAAATATATTTTAGTTAATTTCATCTTCTG	38
62	ACCTAAATTTAATGGTTTGAAATACCGACCGTGTGATA	38
63	AATAAGGCGTTAAATAAGAATAAACACCGGAATCATAA	38
64	TTACTAGAAAAAGCCTGTTTAGTATCATATGCGTTATA	38
65	CAAATTCTTACCAGTATAAAGCCAACGCTCAACAGTAG	38
66	GGCTTAATTGAGAATCGCCATATTTAACAACGCCAACA	38
67	TGTAATTTAGGCAGAGGCATTTTCGAGCCAGTAATAAG	38
68	AGAATATAAAGTACCGACAAAAGGTAAAGTAATTCTGT	38
69	CCAGACGACGACAATAAACAACATGTTCAGCTAATGCA	38
70	GAACGCGCCTGTTTATCAACAATAGATAAGTCCTGAAC	38
71	AAGAAAAATAATATCCCATCCTAATTTACGAGCATGTA	38
72	GAAACCAATCAATAATCGGCTGTCTTTCCTTATCATTC	38
73	CAAGAACGGGTATTAAACCAAGTACCGCACTCATCGAG	38
74	AACAAGCAAGCCGTTTTTATTTTCATCGTAGGAATCAT	38
75	TACCGCGCCCAATAGCAAGCAAATCAGATATAGAAGGC	38
76	TTATCCGGTATTCTAAGAACGCGAGGCGTTTTAGCGAA	38
77	CCTCCCGACTTGCGGGAGGTTTTGAAGCCTTAAATCAA	38
78	GATTAGTTGCTATTTTGCACCCAGCTACAATTTTATCC	38

79	TGAATCTTACCAACGCTAACGAGCGTCTTTCCAGAGCC	38
80	TAATTTGCCAGTTACAAAATAAACAGCCATATTATTTA	38
81	TCCCAATCCAAATAAGAAACGATTTTTTGTTTAACGTC	38
82	AAAAATGAAAATAGCAGCCTTTACAGAGAGAATAACAT	38
83	AAAAACAGGGAAGCGCATTAGACGGGAGAATTAACTGA	38
84	ACACCCTGAACAAAGTCAGAGGGTAATTGAGCGCTAAT	38
85	ATCAGAGAGATAACCCACAAGAATTGAGTTAAGCCCAA	38
86	TAATAAGAGCAAGAAACAATGAAATAGCAATAGCTATC	38
87	TTACCGAAGCCCTTTTTAAGAAAAGTAAGCAGATAGCC	38
88	GAACAAAGTTACCAGAAGGAAACCGAGGAAACGCAATA	38
89	ATAACGGAATACCCAAAAGAACTGGCATGATTAAGACT	38
90	CCTTATTACGCAGTATGTTAGCAAACGTAGAAAATACA	38
91	TACATAAAGGTGGCAACATATAAAAGAAACGCAAAGAC	38
92	ACCACGGAATAAGTTTATTTTGTCACAATCAATAGAAA	38
93	ATTCATATGGTTTACCAGCGCCAAAGACAAAAGGGCGA	38
94	CATTCAACCGATTGAGGGAGGGAAGGTAAATATTGACG	38
95	GAAATTATTCATTAAAGGTGAATTATCACCGTCACCGA	38

96	CTTGAGCCATTTGGGAATTAGAGCCAGCAAAATCACCA	38
97	GTAGCACCATTACCATTAGCAAGGCCGGAAACGTCACC	38
98	AATGAAACCATCGATAGCAGCACCGTAATCAGTAGCGA	38
99	CAGAATCAAGTTTGCCTTTAGCGTCAGACTGTAGCGCG	38
100	TTTTCATCGGCATTTTCGGTCATAGCCCCCTTATTAGC	38
101	GTTTGCCATCTTTTCATAATCAAAATCACCGGAACCAG	38
102	AGCCACCACCGGAACCGCCTCCCTCAGAGCCGCCACCC	38
103	TCAGAACCGCCACCCTCAGAGCCACCACCCTCAGAGCC	38
104	GCCACCAGAACCACCACCAGAGCCGCCGCCAGCATTGA	38
105	CAGGAGGTTGAGGCAGGTCAGACGATTGGCCTTGATAT	38
106	TCACAAACAAATAAATCCTCATTAAAGCCAGAATGGAA	38
107	AGCGCAGTCTCTGAATTTACCGTTCCAGTAAGCGTCAT	38
108	ACATGGCTTTTGATGATACAGGAGTGTACTGGTAATAA	38
109	GTTTTAACGGGGTCAGTGCCTTGAGTAACAGTGCCCGT	38
110	ATAAACAGTTAATGCCCCCTGCCTATTTCGGAACCTAT	38
111	TATTCTGAAACATGAAAGTATTAAGAGGCTGAGACTCC	38
112	TCAAGAGAAGGATTAGGATTAGCGGGGTTTTGCTCAGT	38
113	ACCAGGCGGATAAGTGCCGTCGAGAGGGTTGATATAAG	38
114	TATAGCCCGGAATAGGTGTATCACCGTACTCAGGAGGT	38
115	TTAGTACCGCCACCCTCAGAACCGCCACCCTCAGAACC	38
116	GCCACCCTCAGAGCCACCACCCTCATTTTCAGGGATAG	38
117	CAAGCCCAATAGGAACCCATGTACCGTAACACTGAGTT	38
118	TCGTCACCAGTACAAACTACAACGCCTGTAGCATTCCA	38
119	CAGACAGCCCTCATAGTTAGCGTAACGATCTAAAGTTT	38
120	TGTCGTCTTTCCAGACGTTAGTAAATGAATTTTCTGTA	38
121	TGGGATTTTGCTAAACAACTTTCAACAGTTTCAGCGGA	38
122	GTGAGAATAGAAAGGAACAACTAAAGGAATTGCGAATA	38
123	ATAATTTTTTCACGTTGAAAATCTCCAAAAAAAAGGCT	38
124	CCAAAAGGAGCCTTTAATTGTATCGGTTTATCAGCTTG	38
125	CTTTCGAGGTGAATTTCTTAAACAGCTTGATACCGATA	38
126	GTTGCGCCGACAATGACAACAACCATCGCCCACGCATA	38
127	ACCGATATATTCGGTCGCTGAGGCTTGCAGGGAGTTAA	38
128	AGGCCGCTTTTGCGGGATCGTCACCCTCAGCAGCGAAA	38
129	GACAGCATCGGAACGAGGGTAGCAACGGCTACAGAGGC	38
130	TTTGAGGACTAAAGACTTTTTCATGAGGAAGTTTCCAT	38
131	TAAACGGGTAAAATACGTAATGCCACTACGAAGGCACC	38
132	AACCTAAAACGAAAGAGGCAAAAGAATACACTAAAACA	38
133	CTCATCTTTGACCCCCAGCGATTATACCAAGCGCGAAA	38
134	CAAAGTACAACGGAGATTTGTATCATCGCCTGATAAAT	38
135	TGTGTCGAAATCCGCGACCTGCTCCATGTTACTTAGCC	38
136	GGAACGAGGCGCAGACGGTCAATCATAAGGGAACCGAA	38
137	CTGACCAACTTTGAAAGAGGACAGATGAACGGTGTACA	38
138	GACCAGGCGCATAGGCTGGCTGACCTTCATCAAGAGTA	38
139	ATCTTGACAAGAACCGGATATTCATTACCCAAATCAAC	38
140	GTAACAAAGCTGCTCATTCAGTGAATAAGGCTTGCCCT	38
141	GACGAGAAACACCAGAACGAGTAGTAAATTGGGCTTGA	38
142	GATGGTTTAATTTCAACTTTAATCATTGTGAATTACCT	38
143	TATGCGATTTTAAGAACTGGCTCATTATACCAGTCAGG	38
144	ACGTTGGGAAGAAAAATCTACGTTAATAAAACGAACTA	38
145	ACGGAACAACATTATTACAGGTAGAAAGATTCATCAGT	38
146	TGAGATTTAGGAATACCACATTCAACTAATGCAGATAC	38
147	ATAACGCCAAAAGGAATTACGAGGCATAGTAAGAGCAA	38
148	CACTATCATAACCCTCGTTTACCAGACGACGATAAAAA	38
149	CCAAAATAGCGAGAGGCTTTTGCAAAAGAAGTTTTGCC	38
150	AGAGGGGGTAATAGTAAAATGTTTAGACTGGATAGCGT	38
151	CCAATACTGCGGAATCGTCATAAATATTCATTGAATCC	38
152	CCCTCAAATGCTTTAAACAGTTCAGAAAACGAGAATGA	38
153	CCATAAATCAAAAATCAGGTCTTTACCCTGACTATTAT	38
154	AGTCAGAAGCAAAGCGGATTGCATCAAAAAGATTAAGA	38
155	GGAAGCCCGAAAGACTTCAAATATCGCGTTTTAATTCG	38
156	AGCTTCAAAGCGAACCAGACCGGAAGCAAACTCCAACA	38
157	GGTCAGGATTAGAGAGTACCTTTAATTGCTCCTTTTGA	38
158	TAAGAGGTCATTTTTGCGGATGGCTTAGAGCTTAATTG	38
159	CTGAATATAATGCTGTAGCTCAACATGTTTTAAATATG	38
160	CAACTAAAGTACGGTGTCTGGAAGTTTCATTCCATATA	38
161	ACAGTTGATTCCCAATTCTGCGAACGAGTAGATTTAGT	38
162	TTGACCATTAGATACATTTCGCAAATGGTCAATAACCT	38
163	GTTTAGCTATATTTTCATTTGGGGCGCGAGCTGAAAAG	38
164	GTGGCATCAATTCTACTAATAGTAGTAGCATTAACATC	38
165	CAATAAATCATACAGGCAAGGCAAAGAATTAGCAAAAT	38
166	TAAGCAATAAAGCCTCAGAGCATAAAGCTAAATCGGTT	38
167	GTACCAAAAACATTATGACCCTGTAATACTTTTGCGGG	38
168	AGAAGCCTTTATTTCAACGCAAGGATAAAAATTTTTAG	38
169	AACCCTCATATATTTTAAATGCAATGCCTGAGTAATGT	38
170	GTAGGTAAAGATTCAAAAGGGTGAGAAAGGCCGGAGAC	38
171	AGTCAAATCACCATCAATATGATATTCAACCGTTCTAG	38
172	CTGATAAATTAATGCCGGAGAGGGTAGCTATTTTTGAG	38
173	AGATCTACAAAGGCTATCAGGTCATTGCCTGAGAGTCT	38
174	GGAGCAAACAAGAGAATCGATGAACGGTAATCGTAAAA	38
175	CTAGCATGTCAATCATATGTACCCCGGTTGATAATCAG	38
176	AAAAGCCCCAAAAACAGGAAGATTGTATAAGCAAATAT	38
177	TTAAATTGTAAACGTTAATATTTTGTTAAAATTCGCAT	38
178	TAAATTTTTGTTAAATCAGCTCATTTTTTAACCAATAG	38
179	GAACGCCATCAAAAATAATTCGCGTCTGGCCTTCCTGT	38
180	AGCCAGCTTTCATCAACATTAAATGTGAGCGAGTAACA	38
181	ACCCGTCGGATTCTCCGTGGGAACAAACGGCGGATTGA	38
182	CCGTAATGGGATAGGTCACGTTGGTGTAGATGGGCGCA	38
183	TCGTAACCGTGCATCTGCCAGTTTGAGGGGACGACGAC	38
184	AGTATCGGCCTCAGGAAGATCGCACTCCAGCCAGCTTT	38
185	CCGGCACCGCTTCTGGTGCCGGAAACCAGGCAAAGCGC	38
186	CATTCGCCATTCAGGCTGCGCAACTGTTGGGAAGGGCG	38
187	ATCGGTGCGGGCCTCTTCGCTATTACGCCAGCTGGCGA	38

188	AAGGGGGATGTGCTGCAAGGCGATTAAGTTGGGTAACG	38
189	CCAGGGTTTTCCCAGTCACGACGTTGTAAAACGACGGC	38
190	CAGTGCCAAGCTTGCATGCCTGCAGGTCGACTCTAGAGGATCTTTT	46

For protein detection the desired positions were selected and each oligo was given a 3 thymine overhang conjugated to the binding motif at the 5' end.

1 central biotin binding site (1B)
Oligo no 96 replaced with
5' – biotinTTTCTTGAGCCATTTGGGAATTAGAGCCAGCAAAATCACCA – 3'

3 central biotin binding sites (3B)
Oligo no 95 replaced with
5' – biotinTTTGAAATTATTCATTAAAGGTGAATTATCACCGTCACCGA– 3'

Oligo no 96 replaced with
5' – biotinTTTCTTGAGCCATTTGGGAATTAGAGCCAGCAAAATCACCA – 3'

Oligo no 97 replaced with
5' – biotinTTTGTAGCACCATTACCATTAGCAAGGCCGGAAACGTCACC – 3'

5 central biotin binding sites (5B)
Oligo no 94 replaced with
5' – biotinTTTCATTCAACCGATTGAGGGAGGGAAGGTAAATATTGACG – 3'

Oligo no 95 replaced with
5' – biotinTTTGAAATTATTCATTAAAGGTGAATTATCACCGTCACCGA– 3'

Oligo no 96 replaced with
5' – biotinTTTCTTGAGCCATTTGGGAATTAGAGCCAGCAAAATCACCA – 3'

Oligo no 97 replaced with
5' – biotinTTTGTAGCACCATTACCATTAGCAAGGCCGGAAACGTCACC – 3'

Oligo no 98 replaced with
5' – biotinTTTAATGAAACCATCGATAGCAGCACCGTAATCAGTAGCGA – 3'

3 separated biotin binding sites (Figure 5a in main text)
Oligo no 48 replaced with
5' – biotinTTTAGAAATAAAGAAATTGCGTAGATTTTCAGGTTTAACGT – 3'

Oligo no 96 replaced with
5' – biotinTTTCTTGAGCCATTTGGGAATTAGAGCCAGCAAAATCACCA – 3'

Oligo no 143 replaced with
5' – biotinTTTTATGCGATTTTAAGAACTGGCTCATTATACCAGTCAGG – 3'

The design for binding one digoxigenin was identical as for the biotin design 1B except that a 5' digoxigenin (NHS Ester) was substituted for biotin. The IDT codes for the biotin and digoxigenin modifications are \5Biosg\ and \5DigN\ respectively.

References

(1) Bell, N. A. W.; Thacker, V. V; Hernández-Ainsa, S.; Fuentes-Perez, M. E.; Moreno-Herrero, F.; Liedl, T.; Keyser, U. F. *Lab Chip* **2013**, *13*, 1859–1862.

(2) Böhle, T.; Benndorf, K. *Pflugers Arch.* **1994**, *427*, 487–491.

(3) Hall, J. E. *J. Gen. Physiol.* **1975**, *66*, 531–532.

(4) Kowalczyk, S. W.; Tuijtel, M. W.; Donkers, S. P.; Dekker, C. *Nano Lett.* **2010**, *10*, 1414–1420.